Porous Hollow Fiber Nickel Electrodes for Effective Supply and Reduction of Carbon Dioxide to Methane through Microbial Electrosynthesis

DOI: 10.1002/((adfm.201804860))
Article type: Full paper

Porous Hollow Fiber Nickel Electrodes for Effective Supply and Reduction of Carbon Dioxide to Methane through Microbial Electrosynthesis

*Manal F. Alqahtani, Krishna P. Katuri, Suman Bajracharya, Yuanlie Yu, Zhiping Lai, and Pascal Elias Saikaly**

Manal F. Alqahtani, Krishna P. Katuri, Suman Bajracharya, and Pascal Elias Saikaly
Biological and Environmental Sciences and Engineering (BESE) Division, Water Desalination and Reuse Center, King Abdullah University of Science and Technology, Thuwal 23955-6900, Saudi Arabia

Yuanlie Yu and *Zhiping Lai*
Physical Science and Engineering (PSE) Division, Advanced Membrane and Porous Materials Center, King Abdullah University of Science and Technology, Thuwal 23955-6900, Saudi Arabia

E-mail: pascal.saikaly@kaust.edu.sa;

Keywords: CO_2 reduction, microbial electrosynthesis, porous hollow fiber cathode, waste to resource, electromethanogenesis

Fossil fuels are still considered the primary feedstock for global energy production,[1] with 86% of the global energy used comes from burning fossil fuels,[2] generating 35 billion tons of carbon dioxide (CO_2) annually,[3] resulting in serious environmental pollution and climate change issues.[4] However, fossil fuel resources are finite because they are currently being consumed at a faster rate than they are generated.[5] Moreover, our reliance on fossil fuels for global energy production is expected to continue for the near future[1a, 3] and will increase with the increase in global population, which reached 7.62 billion as of June 2018.[1b, 6] An immediate solution that can relieve our reliance on fossil fuels and decrease the emissions of CO_2, is the sustainable reduction of waste CO_2 to useful chemicals and fuels.[1b, 4, 7]

Various methods including electrocatalysis, photocatalysis, biocatalysis by cyanobacteria, green algae, and some autotrophic bacteria, and chemical transformation through organic reactions, have been proposed in the literature for the conversion of CO_2 into useful products.[1b, 4, 8] Of the different methods studied, electrochemical reduction of CO_2 to useful chemicals such as methane (CH_4), methanol (CH_3OH), ethylene (C_2H_4), ethanol (CH_3CH_2OH), formic acid

(HCOOH), carbon monoxide (CO) etc. appears to be the most promising approach because: (1) the electrocatalytic process can be conducted in ambient conditions with highly controllable reaction step;[1b, 9] (2) the products of electrochemical reduction can be adjusted by varying the reaction parameters;[4] (3) the electrochemical reduction system can be employed for practical application;[4] and (4) the electric power required to drive the system can be obtained from renewable energy sources such as solar or wind.[1b, 4, 9] The latter is attractive because it can solve one of the main issues in the proliferation and development of renewable energy, and that is intermittency, by providing an energy storage solution for intermittent renewable energy sources.[1b]

Among the different products that can be generated from electrochemical reduction of CO_2, CH_4 production is very attractive because: (1) of their high energy density;[4] (2) they are relatively clean burning in combustion engines;[1a, 10] (3) of the advantage of existing infrastructure for natural gas storage, transport and consumption;[1a, 5, 7a, 11] and (4) it can act as an energy carrier for surplus renewable electricity from wind or solar.[5, 11a] However, the electrochemical reduction of CO_2 to CH_4 is faced with the same challenges like every electrocatalytic CO_2 reduction, such as the highly negative potentials of approximately –1.9 V vs NHE (Normal hydrogen electrode) required for bending the linear and extremely stable CO_2 molecule,[1b, 7c] the need for a precious metal catalysts to reduce the overpotential,[10] and the reactions are not sufficiently specific resulting in a mixture of gaseous and liquid products, instead of a single product.[4, 10] Also, in aqueous electrolyte the hydrogen evolution reaction (HER) competes with the CO_2 reduction reaction (CO_2RR), which necessitates the development of very effective catalysts with low activity towards HER.[1b, 12]

Hybrid biosystems, combining inorganic (for HER) and microbial (for CO_2 reduction) catalysts for converting CO_2 to value-added products are recently gaining attention in the scientific community.[7a, 7c, 13] For example, Nichols et al.[7a] combined a biocompatible photo(electro)chemical HER catalyst with an autotrophic obligate anaerobic archaeon,

Methanosarcina barkeri, that uses the in situ generated H_2 for CO_2 reduction to CH_4. A new approach that has emerged in recent years is that of microbial electrosynthesis (MES), which relies on chemolithoautotrophic bacteria or archaea that can uptake electrons directly or indirectly (for example, as H_2 or formate) from the cathode of an electrochemical cell to catalyze the reduction of CO_2 into fuels or value-added chemicals at low potentials.[8, 14] In this regard, MES acts as a hybrid biosystem where the biocompatible material component (cathode) catalyzes the HER to generate H_2 and the microbial component, which forms a biofilm on the cathode, uses these reducing equivalents to fix CO_2. Since MES uses electricity as the energy source, it can be coupled to renewable energy sources such as wind or solar, and in the case of solar it mimics natural photosynthesis where light, water and CO_2 are used to generate chemical products. MES has several advantages compared to electrochemical CO_2 reduction because they utilize live microbial catalysts that are abundant in nature, regenerative, environmentally friendly, and have good selectivity for desired products (e.g., acetate, CH_4).[15]

In MES system, the common method used to deliver CO_2 to chemolithoautorophs on the cathode is through CO_2-gas bubbling.[16] Since CO_2 reduction proceeds via the adsorption of CO_2 molecules at the biocathode, the low solubility of gaseous CO_2 in solution can lead to diffusion and mass-transfer limitations, which affect conversion rate and efficiency of MES.[17] Hence the development of a cathode architecture with a three-phase interface (i.e., between CO_2 gas, cathodic biofilm and electrolyte) is highly desirable. Bubble-less gas exchange hollow fiber membranes (HFM) are effective for delivering gaseous substrate,[18] and they have been used in a variety of applications from photobioreactors,[19] membrane-supported biofilm reactors (MBfR) for water and wastewater treatment,[20] tissue engineering,[21] and development of artificial organs.[22] In MBfR, gaseous substrate is delivered directly from the inside of hollow fibers to a biofilm attached on the outer wall of the HFM. Recently, our group developed electrically conductive, catalytic and porous hollow-fiber cathode (CCPHF) made of metal or polymer for simultaneous recovery of energy as H_2 and clean water from wastewater.[23] The

unique aspect of these cathodes is that, in addition to their role as cathodes for HER, they can also function as a porous membrane for filtration of treated water.

Inspired by the MBfR concept and our CCPHF cathode architecture, here we report for the first time a hybrid biosystem combining biocompatible nickel-based CCPHF (Ni-CCPHF) cathode with enriched CO_2-fixing hydrogenotrophic methanogen community in MES cell (**Scheme 1**) for the conversion of CO_2 to CH_4 with high Faradaic efficiency (77%) and low cathodic potential (–1V vs. Ag/AgCl). The marriage between artificial (the inorganic catalyst) and natural (microbial catalysts) platforms created an advanced functional material with enhanced function over the individual parts when separated. The Ni-CCPHF cathode facilitated direct delivery of CO_2 gas into the biocathode through the pores in the hollow fibers. The enriched hydrogenotrophic methanogen community on the cathode surface can use the H_2 generated from proton reduction at the cathode as a source of reducing equivalent for the reduction of CO_2 to CH_4. The CCPHF cathode architecture in MES has several advantages summarized as follows: (1) the high specific surface area of the CCPHF cathode maximizes the diffusion of CO_2 gas; (2) the small radial dimensions of the hollow fiber cathodes maximizes the surface-area-to-volume ratio, thus solving the issue of cathode packing density for large-scale applications; and (3) direct delivery of CO_2 gas to the biofilm attached on the cathode avoids the gas-liquid mass transfer limitations.

The custom-built Ni-CCPHF cathode fabricated with nickel (Ni) nanoparticles and the relevant characterizations are presented in **Figure S1**. Scanning electron microscope (SEM) image of the Ni-CCPHF cathode (Figure S1a), and its cross-section (Figure S1b) confirm that the cathode had a small radial dimension with outer diameter of ~950 µm and wall thickness of ~80 µm. These features are advantageous for improving specific surface area and packing density of the cathode. The SEM images confirm that the Ni-CCPHF cathode is porous with pore diameter ranging from 1 to 2 µm (Figure S1a, c). Energy dispersive X-ray spectroscopy (EDS) analysis (Figure S1d) revealed that Ni was the most abundant element (≥ 90%) on the

surface. In this study, Ni was used as a cathode material because: 1) it has a lower HER overpotential compared to most other non-noble metal catalysts;[24] 2) it is more stable under alkaline conditions compared to most other non-noble metal catalysts;[25] the local pH at the cathode surface is likely to be alkaline due to water reduction;[24] and 3) most importantly, it is much cheaper compared to precious metal catalysts such as platinum (Pt), which is commonly used as benchmark catalyst for HER in microbial electrochemical systems.[26]

Submerged flat sheet cathodes are typically used in previous MES studies.[27] For scale up, it is challenging to fabricate flat sheet diffusive cathodes for large-scale MES reactors. In contrast, metal-based hollow fiber membranes are easier to fabricate, by adapting manufacturing processes (i.e. phase inversion/sintering method), which are already used in the industry,[28] as well are easier to integrate in modules. It is a known fact in membrane science that hollow fibers are more easily packed than flat sheet membranes. Also, experience from membrane modules show that hollow fiber design achieves higher specific surface area (surface-area-to-volume ratio) than flat sheet design. The average specific surface area or packing density (m^2 membrane surface/m^3 volume) of hollow fiber membrane in commercial modules are reported at 263 m^2 m^{-3} whereas 100 m^2 m^{-3} for flat sheet membranes.[29] The outer diameter (~1 mm) of the hollow fiber membranes used in the current study is within the range of hollow fibers used in practice. With the dimensions (outer diameter of ~1 mm) of the Ni-CCPHF used in our study, the specific surface area can be increased by adding more fibers to the polyethylene tube (4 cm long and 0.8 cm diameter) without increasing reactor volume (270 mL); this could not be achieved with flat sheet electrodes without increasing the volume of the reactor. Also, because they are self-supporting, the hollow-fiber membranes greatly simplify the hardware for fabrication. Whereas flat-sheet diffusive membranes require a porous support, and the reactor configuration might be complex.[30]

The Ni-CCPHF cathode in our study acted as membrane contactor for gas delivery; high gas electrode contact area (as high as ~4000 m^2 m^{-3} of gas in passive delivery) is created due to

the gas delivery from the inner hollow volume. Indeed, the porous nature of the hollow fiber further enhances the interfacial area in the electrode. Although the dimensions of the hollow fiber are of macroscopic level (**Figure S2**), the larger interfacial area can be created due to the porous structure and gas diffusion design, which can promote and enhance mass-transport and functionality of inorganic and microbial catalysts.

The performance of the Ni-CCPHF cathodes for microbial electrochemical CO_2 reduction to CH_4 was tested in two sets of duplicate double-chambered MES reactors (experimental and control 1 reactors; **Figure 1**). The two sets of reactors were operated in parallel for 8 batches under the same environmental and operational conditions (applied potential of – 1.0 V versus Ag/AgCl [– 0.8 V versus SHE; standard hydrogen electrode], 30 ^{o}C temperature, etc.). The average duration of each batch was 6-8 days, except for the acclimation period (first 4 batches), which was 15 days. In the experimental reactors, only one bundle of Ni-CCPHFs was used to serve as both the cathode and gas-transfer membrane to deliver pure CO_2 gas by passive diffusion to the biofilm attached on the surface of the cathode (Figure 1a), whereas in the control 1 reactors, two separate bundles of Ni-CCPHFs were used, with one bundle serving only as a cathode, and another bundle serving only as a gas-transfer membrane to deliver pure CO_2 gas by passive diffusion (Figure 1b). The average reduction current density for the experimental reactors in batch 8 of operation was three times higher (j = – 0.13 ± 0.01 mA cm^{-2}) than control 1 reactors (j = – 0.047 ± 0.005 mA cm^{-2}) (**Figure 2a**), with average Faradaic efficiency (FE) of 77.5 ± 3.0% for the production of CH_4 from CO_2 at a rate of 140 ± 13 mmol m^{-2} d^{-1}. Production of H_2 was also observed at a rate of 286 ± 5 mmol m^{-2} d^{-1} in the experimental reactors. In contrast, the FE for CH_4 was significantly lower (2.9 ± 4% and rate was 3 ± 4 mmol m^{-2} d^{-1}) in control 1 reactors. Although substantial reduction current was produced in the control 1 reactors, the main product generated was H_2 gas at a rate of 200 ± 104 mmol m^{-2} d^{-1}.

In addition to the gaseous products (i.e. CH_4 and H_2), soluble organic compounds (acetate and formate) were also detected in the electrolytes of both sets of reactors (**Table S1**), but at

very low concentrations, and the FE for acetate and formate was ≤ 1%. The rates of formation of acetate (14 ± 15 mmol m^{-2} d^{-1}) and formate (13.4 ± 16.1 mmol m^{-2} d^{-1}) were higher in the experimental reactors than in control 1 reactors (acetate: 2.5 ± 0.5 mmol m^{-2} d^{-1}; formate: 0.1 ± 0.2 mmol m^{-2} d^{-1}). The mixed culture inoculum source, which was used for enriching hydrogenotrophic methanogens, might have also favored the enrichment of other CO_2-fixing microorganisms, which can accept reducing equivalents from the cathode to reduce CO_2 to various end products.[31] However, in the experimental reactors there was high selectivity towards CH_4 production (77.5 ± 3.0%), because the dual-function Ni-CCPHF cathode provided a suitable niche (both reducing equivalents and CO_2 were concurrently available to the biofilm on the cathode) for the enrichment of hydrogenotrophic methanogens on the surface of the cathode. Whereas in the control reactors, the source of electron donor (cathode) was separated from the electron acceptor (CO_2), and this might have limited the growth of methanogens on the cathode due to diffusion and mass-transfer limitation of CO_2. This was supported by quantitative polymerase chain reaction (qPCR) analysis of the cathodic biofilm microbial community at the end of batch 8. The qPCR data targeting the 16S rRNA gene of methanogenic archaea confirmed that members of the order *Methanobacteriales* (genus *Methanobacterium*) were the dominant methanogens (>99%) detected in this study. In general, the dominant methanogens detected on the biocathode of microbial electrochemical systems belong to the hydrogenotrophic methanogen *Methanobacterium*.[11a, 11b, 32] Higher abundance of *Methanobacteriales* was observed on the biocathode of the experimental reactor (4.91±1.2 × 10^6 copies cm^{-2}) than control 1 reactor (Ni-CCPHF bundle serving only as cathode: 0.334±0.47 × 10^6 copies cm^{-2}, and Ni-CCPHF bundle serving as gas-transfer membrane: 0.52±0.73 × 10^6 copies cm^{-2}). Moreover, the higher methanogenic archaea to bacteria ratio (calculated by qPCR) in the cathodic biofilm of the experimental reactor (0.44 ± 0.3) than in the control 1 reactor (< 0.1 on both bundles), suggests that the dual-function Ni-CCPHF cathode provided a suitable niche for the enrichment of methanogens on the cathode.

The SEM images of the Ni-CCPHF cathodes (**Figure 3**) taken at the end of batch 8 indicated that microbial growth was denser on the experimental reactors (Figure 3a, b) than control 1 reactor (Figure 3c, d). Negligible microbial attachment was observed on the Ni-CCPHFs that were used only as a gas-transfer membrane to deliver CO_2 (Figure 3c). A solid layer of inorganic foulant with complete blockage of the pores was observed on the Ni-CCPHFs that were used only as a cathode in the control 1 reactor (Figure 3d). EDS analysis of this solid layer (**Figure S3**) suggests the presence of calcium/magnesium phosphates and calcium/magnesium carbonates precipitates (5.9 At% C, 41.8 At% O, 8.3 At% P, 0.2 At% Ca, and 0.5 At% Mg). The increase in the local pH (i.e., the pH at the interface between cathode surface and electrolyte) due to water reduction ($2H_2O + 2\ e^- \rightarrow H_2 + 2OH^-$) at the cathode may have resulted in the precipitation of carbonates or phosphates on the surface of the cathode in the control 1 reactors. Lei et al.[33] reported inorganic salt (phosphates) precipitation at the cathode due to the rise in the local pH during water reduction. Such precipitation was not observed in the experimental Ni-CCPHFs, which served as both a cathode and gas-transfer membrane to deliver pure CO_2 gas by passive diffusion to the biofilm, possibly because of the dissolution of CO_2 in electrolyte (CO_2 (aq) + $H_2O \leftrightarrow H_2CO_3 \leftrightarrow H^+ + HCO_3^-$), resulting in weak acids (H_2CO_3 and HCO_3^-) that can buffer the increase in local pH.

Confocal laser scanning microscopy (CLSM) image of the experimental reactor Ni-CCPHF cathode cross-section revealed a well-colonized biofilm on the outer surface of the hollow fiber after eight batches of operation (**Figure S4**). It should be noted that none of the gaseous cathodic reduction products (i.e., CH_4 or H_2) were detected in the CO_2 reservoir gasbag connected to the Ni-CCPHF cathode, suggesting that no biological/abiotic reactions were taking place in the inner surface of the Ni-CCPHF cathode.

To further confirm that the CH_4 generated was mainly through microbial CO_2 reduction, the electrochemical behavior of the Ni-CCPHF cathode alone in the absence of microorganisms was tested in a separate reactor (control 2 reactor) under the same conditions as the experimental

reactors. The measured reduction current density of the control 2 reactor was four times lower (j = – 0.03 mA cm^{-2}) than the experimental reactors (Figure 2a), and the main product generated was H_2 from HER at a rate of 139 mmol m^{-2} d^{-1}. Possible gaseous or soluble products from electrochemical reduction of CO_2 were not detected in the abiotic control (i.e., control 2 reactor). These results further confirm that the observed CH_4 in the experimental and control 1 reactors was due to microbial CO_2 reduction by hydrogenotrophic methanogens. The enhanced current density and observed high H_2 yields in the experimental reactor (286 ± 6 mmol m^{-2} d^{-1}) than control 2 reactor (139 mmol m^{-2} d^{-1}) suggest the possibility of direct electron uptake by H_2 producing bacteria (biotic hydrogen evolution) existing along with hydrogenotrophic methanogens in the biocathode. Our qPCR data supports the presence of bacteria in the biocathode of the experimental reactors, however, elucidating their function was not within the scope of this study. Jourdin et al.[34] reported 8-fold higher current densities from a H_2 producing-autotrophic mixed culture bacteria in graphite plate biocathode (– 0.19 mA cm^{-2}) than abiotic control (– 0.023 mA cm^{-2}) at – 0.75 V vs SHE cathode potential. The presence of H_2 producing bacteria such as *Desulfovibrio* with the hydrogenotrophic methanogen *Methanobacterium*, in mixed culture biocathodes were reported in the literature.[10] Members of the genus *Desulfovibrio*, a sulfate reducing bacteria, were reported for catalyzing H_2 production in mixed culture biocathodes.[26, 35] Although the current study was not designed to determine the different routes (direct or indirect) of electron flow at the cathode, from the available data we can speculate that multiple electron flows (direct via biotic H_2 production or indirect via abiotic HER) might have occurred for driving the sustainable reduction of waste CO_2 gas to a useful energy source (i.e., CH_4) (**Figure S5**).

Linear sweep voltammetry (LSV) analysis was conducted at the end of batch 8 for the Ni-CCPHF cathode of the experimental and control 1 reactor (Figure 2b). The reduction current density was higher for the experimental than control 1 cathode at the sweep potential window opted for the LSV analysis. Also, the onset potential for generating reduction current density

was lower for the experimental (– 0.32 V) than control 1 cathode (– 0.47 V) (Figure 2b). However, the magnitude of current density was drastically reduced after detaching the biofilm from the surface of the experimental Ni-CCPHF cathode by sonication followed by rinsing with 0.1 M HCl (data not shown). These observations suggest that the cathodic biofilm of the experimental reactor was playing a key role in improving the cathode performance through reducing the cathode overpotential by 0.15 V against control 1 cathode. The lower overpotential for the experimental cathode than control 1 cathode might also be due to the lack of inorganic precipitates that can block the active surface of the cathode for HER as previously described (Figure 3d). The lowering of cathode overpotential is one of the reasons for observing improvement in the reduction current density for the experimental reactor over the control 1 reactor (Figure 2a).

The growth of a dense biomass without precipitation of inorganic matter on the surface of Ni-CCPHF cathode in the experimental reactors confirms that the dual-function porous hollow fiber cathode enabled a better control of the three-phase interface (i.e., CO_2, cathodic biofilm and electrolyte) where different reactions can take place (i.e., biological: CO_2 reduction and physico-chemical: HER, pH increase, precipitation of ions, etc.). Direct diffusion of CO_2 gas through the pores of the hollow fibers ensured higher CO_2 availability for the proliferation of hydrogenotrophic methanogens. In addition, this cathode architecture provided a sustainable way to buffer the pH increase in the cathode compartment, minimizing inorganic precipitation, which can block the active surface of the cathode for HER. These simultaneous phenomena resulted in high FE for CH_4 production in the experimental reactors compared to control 1 reactors.

To test the effect of CO_2 concentration on the cathodic biofilm electrosynthesis of CH_4, one of the experimental reactors was operated for an additional batch (batch 9) under different CO_2 concentrations (**Table 1**). The other experimental reactor was discontinued after batch 8 of operation due to detaching the biofilm for LSV analysis as previously described. The CO_2 gas

in batch 9 was supplied by passive diffusion through the pores of the Ni-CCPHF cathode as in previous batches except for one of the tests (condition 4) where pure CO_2 gas was supplied in the reactor's headspace rather than through the Ni-CCPHF cathode. The biocathode electrosynthesis activity for CH_4 production was proportional to the feed CO_2 concentration. The CH_4 production rate was improved by four times, with FE of 83% when the CO_2 concentration was increased from 20% (condition 1: 20% CO_2 and 80% N_2) to 100% (condition 2: pure CO_2). This dependency of biocathode electrosynthesis on CO_2 concentration was reconfirmed when the CO_2 concentration was reduced back to 20% (condition 3: 20% CO_2 and 80% N_2), where biocathode electrosynthesis of CH_4 was minimized reaching to values similar to condition 1 (Table 1). In contrast, hydrogen production rates were higher at 20% CO_2 (conditions 1 and 3) than 100% CO_2 (condition 2) (Table 1). The high rates of production and FE for H_2 at low CO_2 concentration (20%) suggests that hydrogenotrophic methanogens were CO_2 limited. The increase in reduction current density was also correlated with the increase in CO_2 concentration (**Figure S6**); the maximum reduction current density was increased by a factor of 1.6, from – 0.11 mA cm^{-2} (condition 1) to – 0.18 mA cm^{-2} (condition 2).

The production rate and FE for CH_4 were significantly lower when CO_2 was supplied through the headspace (condition 4) than through the pores of the Ni-CCPHF cathode (conditions 1 to 3). The diffusion and mass-transfer limitations of CO_2 gas from the reactor headspace to the surface of the submerged biocathode might have reduced the microbial electrochemical CO_2 reduction to CH_4. Also, the reduction current density was drastically reduced from j = – 0.18 mA cm^{-2} in condition 2 (pure CO_2) to j = – 0.025 mA cm^{-2} in condition 4 (pure CO_2) (Figure S6). Although the FE for H_2 production was dominant (84%) in condition 4, it seems that the low CO_2 availability near the cathode affected the H_2 yield too, as the rate of H_2 generated in condition 4 was 1.75 times lower than condition 2 despite the same concentration (100%) of CO_2 was used in both conditions (Table 1). It has been demonstrated that carbonic acid (H_2CO_3) and bicarbonate (HCO_3^-)[36] can reduce cathode overpotential by

299 catalyzing HER on metallic materials, such as stainless steel and nickel, due to their ability to
300 deprotonate easily.[37] Also, Ki et al.[38] showed that addition of CO_2 (100%) to the cathode
301 chamber eliminated pH-related concentration overpotentials in microbial electrolysis cell by
302 decreasing the pH of the electrolyte. Thus, making CO_2 more available to the Ni-CCPHF
303 cathode may enhance reduction current density and rate of H_2 production, and this could explain
304 why the current density and H_2 production was higher in condition 2 than 4. Overall, the
305 observed high reduction current densities and better Faradaic conversions of current to CH_4 in
306 conditions 1, 2 and 3 compared to condition 4 demonstrate that carbon capture and conversion
307 by chemolithoautotrophs was accelerated when CO_2 was supplied directly to the cathodic
308 biofilm using Ni-CCPHF cathode.

309 In conclusion, we have established an efficient hybrid bioinorganic system for CO_2
310 reduction to CH_4 by coupling a new cathode configuration with enriched methanogenic
311 community. Employing Ni-CCPHF as an advanced material with dual function (i.e. acting as a
312 gas-transfer membrane for CO_2 delivery and inorganic electro-catalyst for hydrogen
313 generation) created a suitable niche for increasing the density and activity of biological catalyst
314 (i.e., hydrogenotrophic methanogens). The superior performance of CO_2 reduction to CH_4 with
315 FE of 77% was attributed to the cathode architecture, which enabled a better control of the
316 three-phase interface (CO_2 gas, catholyte and biocathode), mimicking the gas diffusion
317 electrodes used in fuel cells. This cathode architecture can also provide a sustainable way to
318 buffer the local pH at the cathode of microbial electrochemical systems, thus decreasing pH-
319 related concentration overpotentials caused by the increase in local pH due to water reduction.
320 [36, 38] The concept of hybrid bioinorganic system for CO_2 reduction is not only limited to
321 hydrogenotrophic methanogens, but lends itself to other chemolithoautotrophs, such as
322 homoacetogens which can reduce CO_2 to acetate using reducing equivalents from the cathode.
323 Also, the concept of using CCPHF cathode in MES is not limited to metal-based HFMs, but
324 cheaper membranes such as polymeric HFMs can be used to fabricate these types of CCPHF

cathodes, thus minimizing cost of fabrication. For example, porous polymeric hollow fibers can be converted to a cathode by coating them with non-noble metal catalysts using atomic layer deposition method. [8] Most importantly, this cathode architecture makes the MES process highly attractive for on-site carbon capture and utilization of CO_2 gas generated from various industrial sources.

Supporting Information

Supporting Information is available from the Wiley Online Library or from the author.

Acknowledgements

This work was supported by Competitive Research Grant (URF/1/2985-01-01) from King Abdullah University of Science and Technology. We thank Dr. Srikanth Pedireddy for generating Scheme 1, Figure S4 and ToC. Additionally, we acknowledge Mr. Hyun ho Hwang (Heno) at the Office of Academic Writing Services at KAUST for generating Figure 1 in the manuscript.

Received: ((will be filled in by the editorial staff))
Revised: ((will be filled in by the editorial staff))
Published online: ((will be filled in by the editorial staff))

References

[1] a) A. Schoedel, Z. Ji, O. M. Yaghi, *Nat Energy* **2016**, 1; b) A. Vasileff, Y. Zheng, S. Z. Qiao, *Adv Energy Mater* **2017**, 7.
[2] BP, BP Statistical Review of World Energy June 2016, https://www.bp.com/content/dam/bp/pdf/energy-economics/statistical-review-2016/bp-statistical-review-of-world-energy-2016-full-report.pdf, accessed: 08/05/2018.
[3] W. Bank, CO2 emissions https://data.worldbank.org/indicator/EN.ATM.CO2E.KT, accessed: 2018.
[4] W. J. Zhang, Y. Hu, L. B. Ma, G. Y. Zhu, Y. R. Wang, X. L. Xue, R. P. Chen, S. Y. Yang, Z. Jin, *Adv Sci* **2018**, 5.
[5] M. C. A. A. van Eerten-Jansen, N. C. Jansen, C. M. Plugge, V. de Wilde, C. J. N. Buisman, A. ter Heijne, *J Chem Technol Biot* **2015**, 90, 963.
[6] Current World Population Clock http://www.worldometers.info/world-population/, accessed: 21 May, 2018.
[7] a) E. M. Nichols, J. J. Gallagher, C. Liu, Y. D. Su, J. Resasco, Y. Yu, Y. J. Sun, P. D. Yang, M. C. Y. Chang, C. J. Chang, *P Natl Acad Sci USA* **2015**, 112, 11461; b) Y. Song, R. Peng, D. K. Hensley, P. V. Bonnesen, L. B. Liang, Z. L. Wu, H. M. Meyer,

M. F. Chi, C. Ma, B. G. Sumpter, A. J. Rondinone, *Chemistryselect* **2016**, 1, 6055; c) M. Baca, S. Singh, M. Gebinoga, F. Weise, G. Schlingloff, A. Schober, *Adv Energy Mater* **2016**, 6; d) X. C. Kang, Q. G. Zhu, X. F. Sun, J. Y. Hu, J. L. Zhang, Z. M. Liu, B. X. Han, *Chem Sci* **2016**, 7, 266; e) X. F. Sun, X. C. Kang, Q. G. Zhu, J. Ma, G. Y. Yang, Z. M. Liu, B. X. Han, *Chem Sci* **2016**, 7, 2883.

[8] K. P. Katuri, S. Kalathil, A. Ragab, B. Bian, M. F. Alqahtani, D. Pant, P. E. Saikaly, *Adv Mater* **2018**, DOI: 10.1002/adma.201707072e1707072.

[9] a) E. V. Kondratenko, G. Mul, J. Baltrusaitis, G. O. Larrazabal, J. Perez-Ramirez, *Energ Environ Sci* **2013**, 6, 3112; b) J. L. Qiao, Y. Y. Liu, F. Hong, J. J. Zhang, *Chem Soc Rev* **2014**, 43, 631.

[10] M. Siegert, M. D. Yates, D. F. Call, X. P. Zhu, A. Spormann, B. E. Logan, *Acs Sustain Chem Eng* **2014**, 2, 910.

[11] a) M. C. A. A. Van Eerten-Jansen, A. B. Veldhoen, C. M. Plugge, A. J. M. Stams, C. J. N. Buisman, A. Ter Heijne, *Archaea* **2013**, DOI: Unsp 481784 10.1155/2013/481784; b) M. Siegert, M. D. Yates, A. M. Spormann, B. E. Logan, *Acs Sustain Chem Eng* **2015**, 3, 1668; c) H. Hashiba, H. K. Sato, S. Yotsuhashi, K. Fujii, M. Sugiyama, Y. Nakano, *Sustain Energ Fuels* **2017**, 1, 1734.

[12] R. Daiyan, X. Y. Lu, Y. H. Ng, R. Amal, *Chemistryselect* **2017**, 2, 879.

[13] B. C. C. Chong Liu, Marika Ziesack,, D. G. N. Pamela A. Silver, *Science* **2016**, 352, 1210.

[14] a) K. P. Nevin, T. L. Woodard, A. E. Franks, Z. M. Summers, D. R. Lovley, *Mbio* **2010**, 1; b) S. Bajracharya, S. Srikanth, G. Mohanakrishna, R. Zacharia, D. P. B. T. B. Strik, D. Pant, *J Power Sources* **2017**, 356, 256.

[15] K. Rabaey, R. A. Rozendal, *Nat Rev Microbiol* **2010**, 8, 706.

[16] L. Jourdin, Y. Lu, V. Flexer, J. Keller, S. Freguia, *Chemelectrochem* **2016**, 3, 581.

[17] S. Bajracharya, K. Vanbroekhoven, C. J. N. Buisman, D. Pant, D. P. B. T. B. Strik, *Environ Sci Pollut R* **2016**, 23, 22292.

[18] H. W. Kim, A. K. Marcus, J. H. Shin, B. E. Rittmann, *Environ Sci Technol* **2011**, 45, 5032.

[19] a) M. Kalontarov, D. F. R. Doud, E. E. Jung, L. T. Angenent, D. Erickson, *Rsc Adv* **2013**, 3, 13203; b) M. Kalontarov, D. F. R. Doud, E. E. Jung, L. T. Angenent, D. Erickson, *Rsc Adv* **2014**, 4, 1460.

[20] a) B. E. Rittmann, *Water Sci Technol* **2006**, 53, 219; b) K. J. Martin, R. Nerenberg, *Bioresource Technol* **2012**, 122, 83.

[21] D. Mohebbi-Kalhori, A. Behzadmehr, C. J. Doillon, A. Hadjizadeh, *J Artif Organs* **2012**, 15, 250.

[22] A. A. Palakkan, D. K. Raj, J. Rojan, R. G. S. Raj, P. R. A. Kumar, C. V. Muraleedharan, T. V. Kumary, *Tissue Eng Pt A* **2013**, 19, 1056.

[23] a) K. P. Katuri, N. M. S. Bettahalli, X. B. Wang, G. Matar, S. Chisca, S. P. Nunes, P. E. Saikaly, *Adv Mater* **2016**, 28, 9504; b) K. P. Katuri, C. M. Werner, R. J. Jimenez-Sandoval, W. Chen, S. Jeon, B. E. Logan, Z. P. Lai, G. L. Arny, P. E. Saikaly, *Environ Sci Technol* **2014**, 48, 12833.

[24] A. W. Jeremiasse, H. V. M. Hamelers, M. Saakes, C. J. N. Buisman, *Int J Hydrogen Energ* **2010**, 35, 12716.

[25] M. H. Miles, *J Electroanal Chem* **1975**, 60, 89.

[26] C. M. Werner, K. P. Katuri, A. R. Hari, W. Chen, Z. Lai, B. E. Logan, G. L. Amy, P. E. Saikaly, *Environ Sci Technol* **2016**, 50, 4439.

[27] a) L. Jourdin, S. Freguia, B. C. Donose, J. Chen, G. G. Wallace, J. Keller, V. Flexer, *J Mater Chem A* **2014**, 2, 13093; b) N. Aryal, A. Halder, P. L. Tremblay, Q. J. Chi, T. Zhang, *Electrochimica Acta* **2016**, 217, 117.

[28] R. W. Baker, *Membrane Technology and Applications*, John Wiley & Sons, Ltd., **2004**.
[29] S.-H. Yoon, in *Membrane Bioreactor Processes: Principles and Applications*, CRC Press **2016**, p. 132.
[30] P. T. Cardew, M. S. le, in *Membrane Processes: A Technology Guide*, DOI: 10.1039/9781847551344-00003, The Royal Society of Chemistry **1998**, p. 3.
[31] C. W. Marshall, D. E. Ross, E. B. Fichot, R. S. Norman, H. D. May, *Appl Environ Microb* **2012**, 78, 8412.
[32] G. Y. Zhen, T. Kobayashi, X. Q. Lu, K. Q. Xu, *Bioresource Technol* **2015**, 186, 141.
[33] Y. Lei, M. Saakes, R. D. van der Weijden, C. J. N. Buisman, *Chemical Engineering Journal* **2018**, 342, 350.
[34] L. Jourdin, S. Freguia, B. C. Donose, J. Keller, *Bioelectrochemistry* **2015**, 102, 56.
[35] F. Aulenta, L. Catapano, L. Snip, M. Villano, M. Majone, *Chemsuschem* **2012**, 5, 1080.
[36] E. Roubaud, R. Lacroix, S. Da Silva, A. Bergel, R. Basséguy, B. Erable, *Electrochimica Acta* **2018**, 275, 32.
[37] S. Da Silva, R. Basseguy, A. Bergel, *Electrochimica Acta* **2004**, 49, 4553.
[38] D. Ki, S. C. Popat, C. I. Torres, *Chemical Engineering Journal* **2016**, 287, 181.

Figure and Scheme Legends

Scheme 1. A schematic of a microbial electrosynthesis (MES) reactor showing the replacement of conventional submerged flat cathode with electrically conductive, catalytic and porous hollow-fiber (CCPHF) cathode. The CCPHF cathode acts as an inorganic electro-catalyst for hydrogen generation from proton reduction and as a gas-transfer membrane for direct CO_2 delivery to CO_2-fixing hydrogenotrophic methanogens (biological catalyst) on the cathode through the pores of the hollow fibers. Water oxidation reaction occuring at the anode supplies the electrons for the hydrogen evolution reaction at the cathode of MES. Hydrogenotrophic methanogens utilize the hydrogen generated at the cathode as a source of reducing equivalents for the conversion of CO_2 to CH_4.

Figure 1. Schematic diagram of (A) experimental and (B) control 1 microbial electrosynthesis (MES) reactors used in this study. 1) Anode compartment; 2) Cathode compartment; 3) Reference electrode; 4) Potentiostat; 5) Gasbag for collecting O_2; 6) Gasbag for passive delivery of CO_2; 7) Gasbag for collecting CH_4. In the experimental reactor (Figure 1a), the Ni-CCPHF bundle served as both, a cathode to provide reducing equivalents and a gas-transfer membrane to deliver CO_2 directly by passive diffusion. In the control 1 reactor (Figure 1b), two separate Ni-CCPHF bundles were used. One of the Ni-CCPHF bundles acted as a cathode to provide reducing equivalents, and the second bundle was used as a gas-transfer membrane to deliver CO_2. One of the Ni-CCPHF bundles connected to the orange wire acted as a cathode to provide reducing equivalents, and the second bundle connected to the CO_2 gasbag was used as a gas-transfer membrane to deliver CO_2.

Figure 2. (A) Average amperometric current density (normalized to the projected surface area of the cathode) generation over time in batch 8 of operation for the experimental and control reactors. In the experimental reactors, the Ni-CCPHF bundle served simultaneously as a cathode and gas-transfer membrane to deliver pure CO_2 gas through passive diffusion (Figure 1a). In the control 1 reactors, two separate Ni-CCPHF bundles were used. One bundle acted as a cathode, and the second bundle was used as a gas-transfer membrane to deliver pure CO_2 gas through passive diffusion (Figure 1b). The abiotic control reactor (i.e. control 2 reactor) was operated similarly to the experimental reactors, except no microbial inoculum was added to the cathode chamber; (B) linear sweep voltammetry (LSV) with a scan rate of 1 mV s^{-1} for the cathodes from the experimental and control 1 reactor. Inset was added to clearly show the onset overpotential for the different cathodes. Pure CO_2 gas was delivered passively without making bubbles so that the system remained undisturbed during electrochemical measurement.

Figure 3. Scanning electron microscope (SEM) images taken at the end of batch 8 for the cathodic biofilms developed on Ni-CCPHF cathode of experimental reactor (A and B) and control 1 reactor (C - Ni-CCPHF that was used only as a gas-transfer membrane for CO_2 delivery, and D - Ni-CCPHF cathode that served only as a cathode).

476 **Table 1.** Summary of methane and hydrogen production rates and corrosponding Faradaic
477 efficiencies in batch 9 of the experimental reactor.

Experimental conditions	Measured CH_4 production rate (mmol m^{-2} d^{-1})	Measured H_2 production rate (mmol m^{-2} d^{-1})	Faradaic efficiency for CH_4 (%)	Faradaic efficiency for H_2 (%)
Condition 1 (20% CO_2)	36.9	350.5	24.3	68.0
Condition 2 (100% CO_2)	161.0	159.5	83.9	20.8
Condition 3 (20% CO_2)	48.8	285.7	30.6	82.1
Condition 4 (100% CO_2)[1]	5.9	90.9	21.8	84.1

478 [1]Condition 4: pure CO_2 gas was supplied in the reactor's headspace rather than through the pores of the Ni-
479 CCPHF cathode.
480
481
482

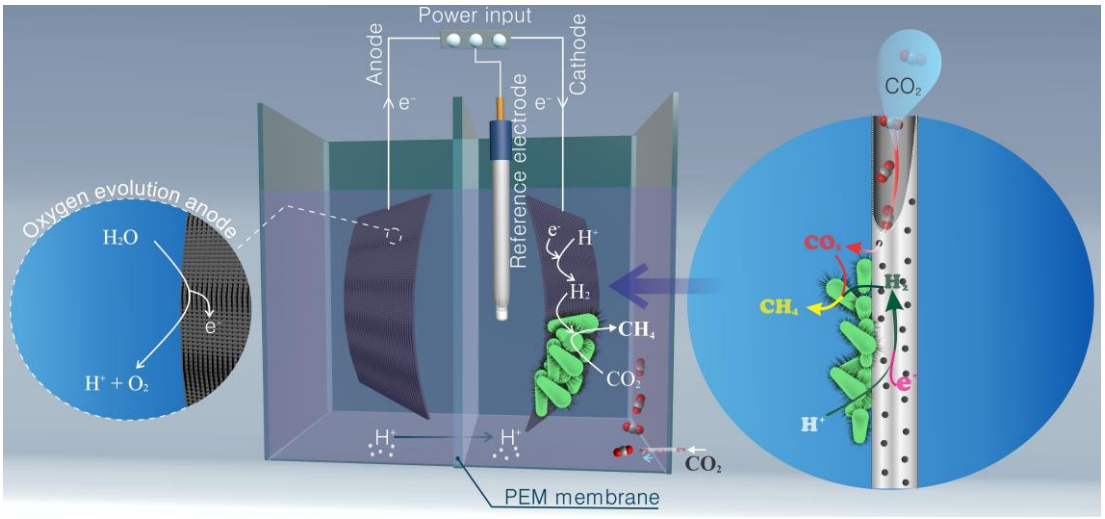

Scheme 1. A schematic of a microbial electrosynthesis (MES) reactor showing the replacement of conventional submerged flat cathode with electrically conductive, catalytic and porous hollow-fiber (CCPHF) cathode. The CCPHF cathode acts as an inorganic electro-catalyst for hydrogen generation from proton reduction and as a gas-transfer membrane for direct CO_2 delivery to CO_2-fixing hydrogenotrophic methanogens (biological catalyst) on the cathode through the pores of the hollow fibers. Water oxidation reaction occuring at the anode supplies the electrons for the hydrogen evolution reaction at the cathode of MES. Hydrogenotrophic methanogens utilize the hydrogen generated at the cathode as a source of reducing equivalents for the conversion of CO_2 to CH_4.

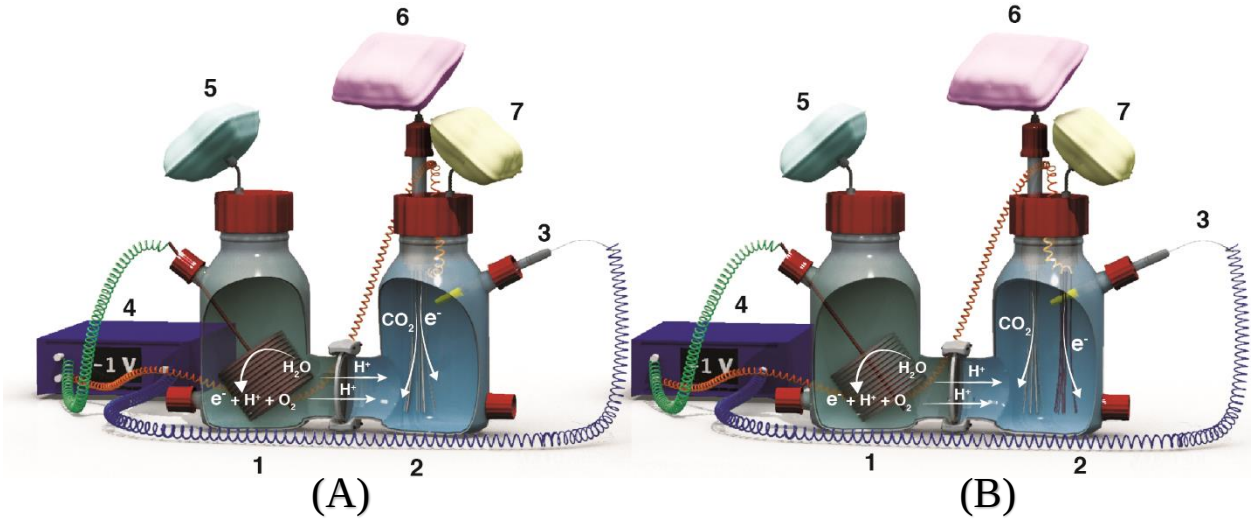

Figure 1. Schematic diagram of (A) experimental and (B) control 1 microbial electrosynthesis (MES) reactors used in this study. 1) Anode compartment; 2) Cathode compartment; 3) Reference electrode; 4) Potentiostat; 5) Gasbag for collecting O_2; 6) Gasbag for passive delivery of CO_2; 7) Gasbag for collecting CH_4. In the experimental reactor (Figure 1a), the Ni-CCPHF bundle served as both, a cathode to provide reducing equivalents and a gas-transfer membrane to deliver CO_2 directly by passive diffusion. In the control 1 reactor (Figure 1b), two separate Ni-CCPHF bundles were used. One of the Ni-CCPHF bundles acted as a cathode to provide reducing equivalents, and the second bundle was used as a gas-transfer membrane to deliver CO_2. One of the Ni-CCPHF bundles connected to the orange wire acted as a cathode to provide reducing equivalents, and the second bundle connected to the CO_2 gasbag was used as a gas-transfer membrane to deliver CO_2.

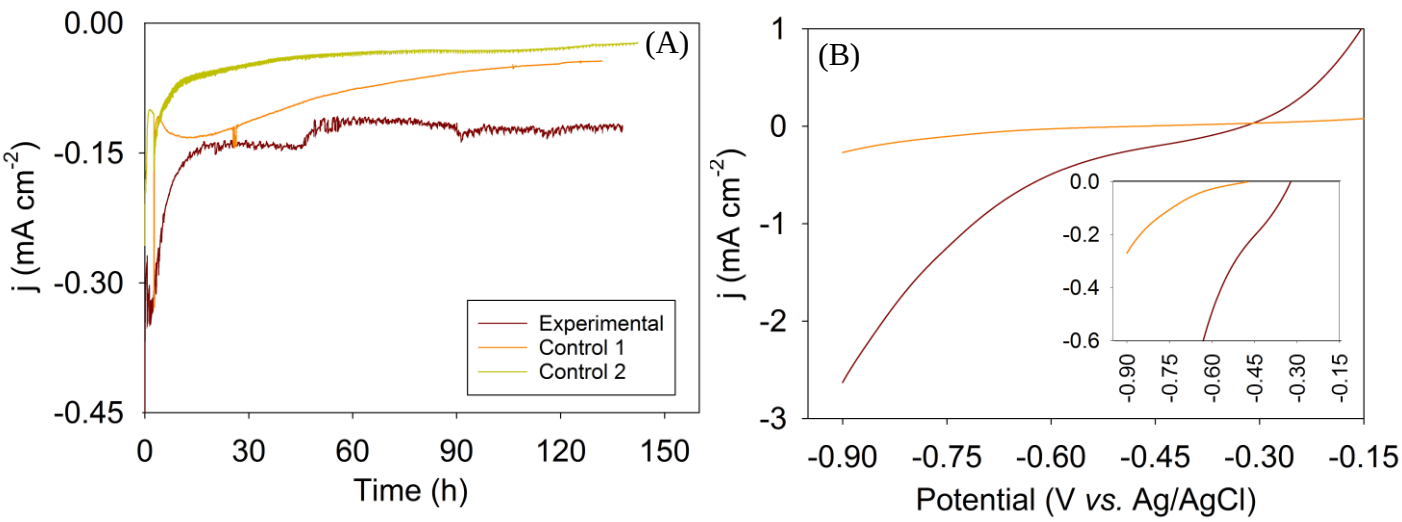

Figure 2. (A) Average amperometric current density (normalized to the projected surface area of the cathode) generation over time in batch 8 of operation for the experimental and control reactors. In the experimental reactors, the Ni-CCPHF bundle served simultaneously as a cathode and gas-transfer membrane to deliver pure CO_2 gas through passive diffusion (Figure 1a). In the control 1 reactors, two separate Ni-CCPHF bundles were used. One bundle acted as a cathode, and the second bundle was used as a gas-transfer membrane to deliver pure CO_2 gas through passive diffusion (Figure 1b). The abiotic control reactor (i.e. control 2 reactor) was operated similarly to the experimental reactors, except no microbial inoculum was added to the cathode chamber; (B) linear sweep voltammetry (LSV) with a scan rate of 1 mV s^{-1} for the cathodes from the experimental and control 1 reactor. Inset was added to clearly show the onset overpotential for the different cathodes. Pure CO_2 gas was delivered passively without making bubbles so that the system remained undisturbed during electrochemical measurement.

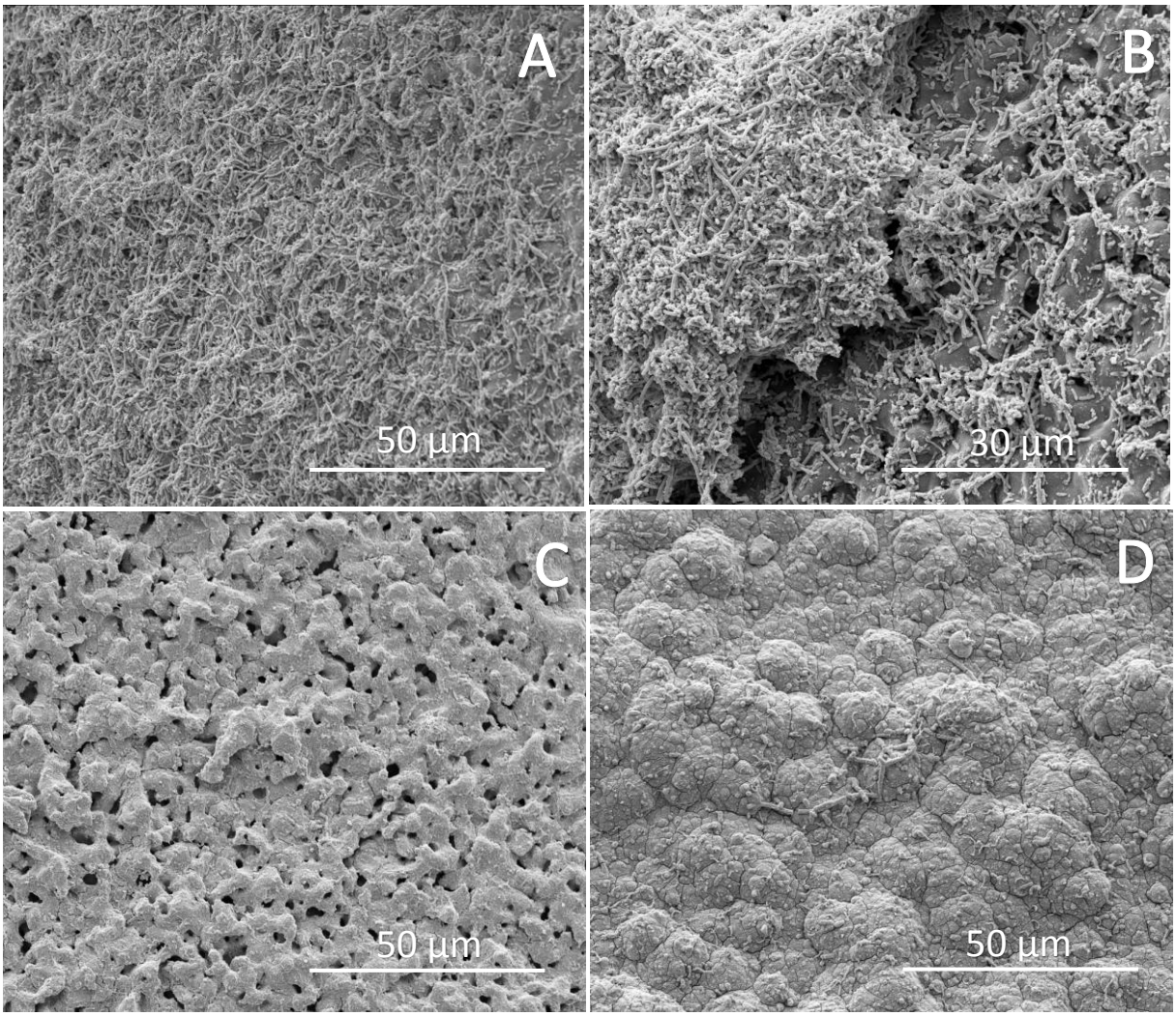

Figure 3. Scanning electron microscope (SEM) images taken at the end of batch 8 for the cathodic biofilms developed on Ni-CCPHF cathode of experimental reactor (A and B) and control 1 reactor (C - Ni-CCPHF that was used only as a gas-transfer membrane for CO_2 delivery, and D - Ni-CCPHF cathode that served only as a cathode).

Table of Contents

Nickel-based conductive, catalytic and porous hollow fiber for effective microbial electrochemical reduction of CO_2 to methane; hence addressing two challenges facing society in the current century (i.e., energy crisis and global warming).

Keywords: CO_2 reduction, microbial electrosynthesis, porous hollow fiber cathode, waste to resource, electromethanogenesis

M. F. Alqahtani, K. P. Katuri, S. Bajracharya, Y. Yu, Z. Lai, and P. E. Saikaly*

Porous Hollow Fiber Nickel Electrodes for Effective Supply and Reduction of Carbon Dioxide to Methane through Microbial Electrosynthesis

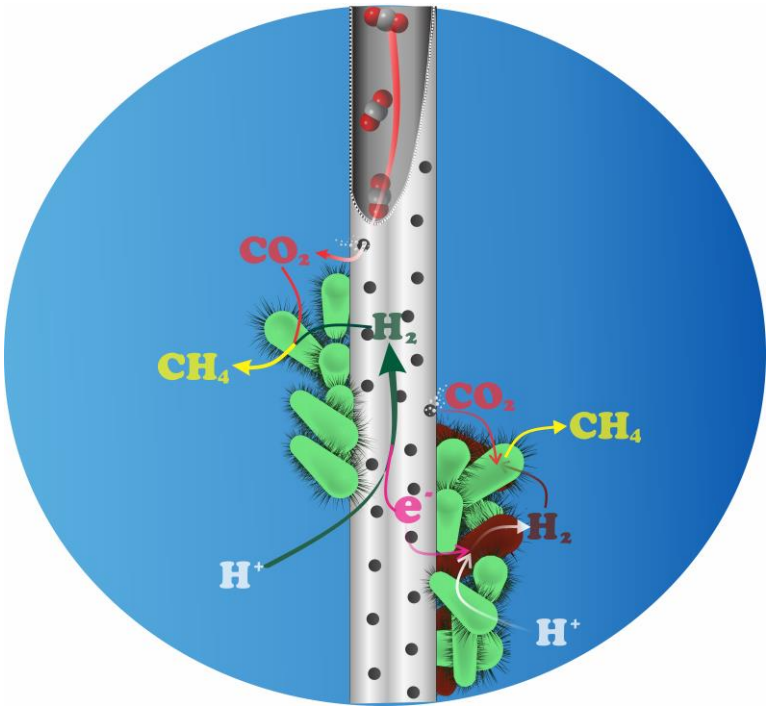

Supporting Information

Porous Hollow Fiber Nickel Electrodes for Effective Supply and Reduction of Carbon Dioxide to Methane through Microbial Electrosynthesis

*Manal F. Alqahtani, Krishna P. Katuri, Suman Bajracharya, Yuanlie Yu, Zhiping Lai, and Pascal Elias Saikaly**

Experimental Section

Fabrication of nickel-based electrically conductive, catalytic and porous hollow-fiber (Ni-CCPHF) cathode: The Ni-CCPHF cathodes having an average pore size of 1-2 μm (Figure S1) were fabricated through combined phase-inversion/sintering method.[1] In brief, nickel powders (~3 μm particles), *N*-methyl-2-pyrrolidinone (NMP, HPLC grade, 99.5%, Alfa Aesar), polyether sulfone (PES, Ultrason® E6020P, BASF) and polyvinylpyrrolidone (PVP, Alfa Aesar) were mixed and well dispersed by ball milling for 18 h, followed by degassing under vacuum for 24 h. Then, the suspension was extruded through a spinneret using water as the inner and outer coagulant. The skeleton of the formed hollow fibers was dried at room temperature and then sintered at 560 °C for 6 h to remove organic compounds under air-flow (500 mL/min). After cooling to room temperature, the hollow fibers were heated at 810 °C for 6 h under pure H_2 environment (pumped at a flow rate of 500 mL/min), to reduce the Ni-CCPHF cathode from the metal oxide to the metal state.

Preparation of Ni-CCPHF cathode bundle: The cathode was configured using eight Ni-CCPHFs (10 cm long each with an outer diameter of 0.09 cm) assembled into a single bundle (Figure S2). One of the ends of the Ni-CCPHF cathode bundle was placed in one polyethylene tube (4 cm long and 0.8 cm diameter) housing, and electrical connection was established between the hollow fibers by filling the gaps with conductive silver epoxy. An insulated stainless-steel wire (0.08 cm diameter) was attached to the Ni-CCPHF bundle (using conductive silver epoxy) as a current collector for the cathode-assembly. Nonconductive epoxy was applied as an additional layer around the conductive silver epoxy to avoid the contact of silver with the

electrolyte during the reactor operation. The other end of each Ni-CCPHF opening was filled with epoxy glue. Approximately 2 cm of each fiber was embedded in the electrical gluing, leaving an active surface area of 2.27 cm^2 per fiber and a cathodic specific surface area of 6.7 m^2 m^{-3} (based on electrolyte volume of 270 ml).

Microbial electrosynthesis (MES) reactor construction and operation: A schematic representation of the reactor is presented in Figure 1. Two-chambered electrochemical cell constructed from borosilicate glass bottle were used for the experiments. Anode and cathode chambers were separated by Nafion® 117 membrane (Sigma, USA). The total and working volume of each chamber was 300 mL and 270 mL, respectively. The cathode chamber has a screw cap on the top with appropriate ports for positioning the Ni-CCPHF cathode bundle, current collector and gasbags (Calibrate, Inc., USA). Additional ports were positioned on the wall of the cathode chamber for inserting the reference electrode (BASi, USA), headspace gas measurements (not shown in Figure 1 for simplicity) and for the replacement of electrolyte. The anode chamber also has a screw cap on the top with an appropriate port for positioning the gasbag. Additional ports were positioned on the wall of the anode chamber for connecting the anode to the potentiostat (VMP3, BioLogic Science Instruments), and for replacement of electrolyte. Activated carbon fiber brush electrode (Mill-Rose, USA), heated at 450 °C for 15 min, was used as the anode. Both the anode and cathode were positioned parallel to the Nafion® 117 membrane.

Two types of MES reactors (experimental and control 1), were constructed in duplicate and operated in parallel under the same conditions. In the experimental reactors, the Ni-CCPHF bundle cathode served as a cathode to provide reducing equivalents for hydrogenotrophic methanogens and as a gas-transfer membrane to deliver CO_2 directly by passive diffusion to methanogenic biofilm attached on the surface of the cathode (Figure 1a). In the control 1 reactors, two separate Ni-CCPHF cathode bundles having equivalent surface area were

positioned parallel to each other at a distance of 4 cm in the cathode chamber. One of the Ni-CCPHF cathode bundles acted as a cathode to provide reducing equivalents for hydrogenotrophic methanogens, and the second bundle was used as a gas-transfer membrane to deliver CO_2 (Figure 1b).

The reactors were operated in fed-batch mode at 30 °C under a cathode set potential of –1.0 V vs. Ag/AgCl using a potentiostat (VMP3, BioLogic Science Instruments). Buffered synthetic mineral medium containing (g L^{-1}): NH_4Cl, 1.5; Na_2HPO_4, 0.6, KCl, 0.1 and 2.5, Na_2HCO_3; and trace minerals and vitamin solutions, was used as the electrolyte (conductivity: 5.62 mS cm^{-1} and pH 7.0) in both compartments.[2] Enriched hydrogenotrophic methanogen community was used as the inoculum (see below) to start the experimental and control 1 reactors. For the first four batches, the experimental and control 1 reactors were supplemented with the inoculum (10 % v/v) to allow enough time for microbial communities to acclimatize and form a biofilm on the cathode for driving the CO_2 reduction. Following this acclimatization period, subsequent batch cycles were fed only with the synthetic medium without any inoculum. Also, for the first four batches, the cathode chamber was operated under H_2:CO_2 (20:80) environment, and for the rest of the batches, only pure CO_2 gas was supplied, unless stated otherwise. Throughout the experimental period, CO_2 gas was supplied through passive diffusion from the inside of hollow fibers (gas phase) to the outside (liquid phase) through the pores of the Ni-CCPHF cathode. To allow CO_2 gas to diffuse passively through the pores of the Ni-CCPHF cathode, the other end of the polyethylene tube housing, used for making the Ni-CCPHF cathode bundle, was connected to a gas reservoir (250 ml gasbag) through a tube connector. Precaution was taken to ensure that all connections were well sealed with nonconductive epoxy/Teflon tape wherever necessary.

In addition, an abiotic control reactor (control 2), with no addition of inoculum, was operated to assess the contribution of abiotic reactions from the cathode under set potential on the process performance. The abiotic reactor was operated similarly to the experimental reactors,

except no microbial inoculum was added to the cathode chamber.

Inoculum: Anaerobic sludge (Manfouha Wastewater Treatment Plant, Riyadh, KSA) was used for the enrichment of hydrogenotrophic methanogens in a closed serum bottle (1 L) under H_2:CO_2 (20:80) environment. The growth synthetic medium described above was used for the enrichment process. Concentrated anaerobic sludge (100 mL) was added to the serum bottle containing 500 mL of oxygen-free growth medium under N_2 environment (anaerobic glove box, Coy laboratories, USA), and sealed with butyl rubber. The headspace of the serum bottle was flushed for 10 min with a mixed gas containing H_2:CO_2 (20:80). Then this bottle was subjected for continuous mixing in a shaking incubator at 30 °C for two months. Once every five days, the headspace of the serum bottle was flushed with H_2:CO_2 (20:80), and once every 10 days, the supernatant solution (i.e. fermented broth above the settled biomass) in the serum bottle was replaced with fresh oxygen-free growth medium. After two months of enrichment, a good stoichiometric conversion of H_2 to CH_4 (> 90%) was observed, and the enriched biomass was harvested for subsequent inoculation of the MES reactors.

Scanning electron microscopy (SEM): ~1 cm long pieces of biofilm-covered Ni-CCPHFs were soaked in 2% glutaraldehyde solution containing phosphate buffer (50 mM, pH 7.0) and stored at 4 °C for 2 days. Then, the samples were incubated overnight with 0.2% osmium tetra oxide solution. Followed by washing with phosphate buffer, the samples were dehydrated in serial graded ethanol solutions. After drying, the samples were fixed on aluminum metal stub using double side cupper tape. Then the samples were coated by gold/palladium for 30 seconds at 25 mA current using sputter coating apparatus under argon atmosphere. Scanning electron micrographs were visualized using Quanta 600D (FEI, The Netherlands). Virgin Ni-CCPHF cathode was subjected directly for imaging without any metal coating.

Energy-dispersive X-ray spectroscopy (EDS): The EDS detector on Quanta 600D FEI and ZEISS Merlin 61-95 SEM (accelerating voltage 20KV and spot-size 6) was switched to

681 determine the elemental composition of the Ni-CCPHF outer surface. Elemental peaks were
682 identified using the built-in software and the atomic (At) % of each element was analyzed over
683 the scanned area.

684 *Confocal laser scanning microscopy (CLSM):* ~1 cm long piece of biofilm-covered Ni-CCPHF
685 from experimental reactor was prepared for confocal imaging. Prior to CLSM imaging, the
686 biofilm on the surface of Ni-CCPHF was washed in phosphate buffer (0.1 M, pH 7.0) and
687 stained by incubating for 15 min in 1 mL of phosphate buffer (0.1 M, pH 7.0) containing 1.5
688 µL of Syto 9 (Invitrogen Corp., Carlsbad, CA) under dark conditions.[2] A Zeiss LSM 510
689 Axiovert Inverted CLSM with a 40× Achroplan oil immersion lens was used to image the
690 biofilm. Images were obtained using an excitation wavelength of 488 nm and a BP500-550
691 emission filter, for green fluorescence.

692 *Electrochemical Analysis:* Electrochemical measurements and recordings were carried out
693 using VMP3 BioLogic potentiostat using three-electrode setup. Chronoamperomentry at –1 V
694 vs Ag/AgCl and linear sweep voltammetry (LSV) at a scan rate of 1 mV s^{-1} were conducted.

695 *Analytical measurements:* Volatile fatty acids (VFAs) and gas composition (H_2, CH_4, and CO_2)
696 were analyzed according to chromatography methods described previously.[3] At the end of
697 each batch cycle, gas samples from the headspace and gasbags were collected by airtight
698 syringe for analysis of gas composition by gas chromatography (GC; model 310, SRI
699 Instruments) equipped with a thermal conductivity detector according to Hari et al.[3b] A 1.83
700 m molecular sieve packed 5A column and argon gas as carrier was used for measuring H_2 and
701 CH_4 concentrations, and a 0.91 m silica gel column and helium gas as carrier was used for
702 measuring CO_2 concentration. The total volumes of the gases were calculated as described
703 previously.[3a] Liquid samples were taken from the cathode chamber and filtered through a
704 0.20-um pore diameter syringe filters prior to VFA measurements. The VFAs were analyzed
705 using ion chromatography (IC, Dionex ICS-3000), equipped with a high-performance

conductivity detector and AS11 column. The samples were introduced through the column for separation by the mobile phase deionized water and KOH.

Quantitative polymerase chain reaction (qPCR): Five 1-cm long Ni-CCPHFs were sampled and placed in a sterile centrifuge tubes containing 3 ml of sterile media and vigorously vortexed to detach biofilm from the surface of the cathode. DNA was extracted from aliquots (250 µl) of samples using the PowerSoil™ DNA extraction kit (MO BIO Laboratories Inc., USA) as per the manufacturer's instructions, and quantified using a NanoDrop spectrophotometer (Thermo Scientific).

To quantify the abundance of total Bacteria, total Archaea and various methanogenic Archaea (*Methanobacteriales*, *Methanomicrobiales*, *Methanosarcinaceae* and *Methanosaetaceae*), qPCR was performed in a 25-µL reaction volume containing 12.5 µL of 2 × iQ Supermix (Bio-Rad Laboratories, Hercules, CA), 0.5 µM of each primer, 0.2 µM of each probe, 1 µl sample DNA, and RNase-free sterile water to a final volume of 25 µL. Amplification was performed using the CFX96 real-time PCR detection system (Bio-Rad Laboratories, Hercules, CA) with PCR conditions described by Ritalahti et al.[4] and Yu et al.[5] All primers, probes and plasmid standards used in this study are listed in Table S2. For each qPCR run, a negative (no template) control was used to test for false positives or contamination. The genomic DNA from each sample was amplified in triplicate. For standard clone preparation, the PCR amplicons were first cloned into a TOPO cloning vector (pCR 2.1-Topo vector, Invitrogen, Carlsbad, CA) according to the manufacturer's protocol. Plasmids from transformed cells were extracted by the PureYield^{TM} Plasmid Miniprep System (Promega, Madison, WI). Copy number per microliter was calculated from the mass concentration and molecular weight of each extracted plasmid DNA. Standard template DNA was 10-fold diluted in series and the threshold cycle (C_t) values for each dilution were plotted against the concentration of each dilution to construct the standard curves.

731 The total gene copy number in the buffer (30 μL) used for eluting extracted DNA was
732 normalized to the total surface area of the Ni-CCPHFs used for extracting DNA, and the results
733 were presented as copies cm^{-2} of cathode

734 *Calculations of Faradaic efficiencies:* Using the ideal gas law equation, the moles (n) of gas
735 generated from the measured gas volume were estimated.

736 $$n\ (mol) = \frac{pV}{RT} \qquad \text{Equation (1)}$$

737 Where p is gas pressure (1 atm), V is the volume of the gas in L, which was calculated from the
738 GC gas composition measurement, T is the temperature (298 K) and R is the gas constant
739 (0.08206 L atm K^{-1} mol^{-1}). The Faradaic efficiency (FE) for the different products was
740 calculates as follows:

741 $$FE\ (H_2)\ \% = \frac{n_{H_2}(mol)*2F}{\int_{t=0}^{t} Idt} \times 100 \qquad \text{Equation (2)}$$

742 $$FE\ (CH_4)\ \% = \frac{n_{CH_4}(mol)*8F}{\int_{t=0}^{t} Idt} \times 100 \qquad \text{Equation (3)}$$

743 $$FE\ (acetate,\ CH_3COOH)\ \% = \frac{n_{CH_3COOH}(mol)*8F}{\int_{t=0}^{t} Idt} \times 100 \qquad \text{Equation (4)}$$

744 $$FE\ (formate,\ HCOOH)\ \% = \frac{n_{HCOOH}(mol)*2F}{\int_{t=0}^{t} Idt} \times 100 \qquad \text{Equation (5)}$$

745 Where n_{H2} and n_{CH4} are the number of moles of hydrogen and methane calculated from Eq 1.
746 The $n_{CH3COOH}$ and n_{HCOOH} were calculated from acetate and formate production measured by IC
747 as described above. I is the current (A), 2 is the moles of electrons needed to produce one mole
748 of hydrogen or formate, 8 is the moles of electrons needed to produce one mole of methane or
749 acetate, F is Faraday's constant F=96485 C/mol e^-, and dt (s) is the time over which the data
750 was analyzed.

751

752 **Table S1.** Concentration of different volatile fatty acids determined by ion chromatography.

Reactors	Acetate (μM)	Formate (μM)	Propionate (μM)	n-Butyrate (μM)
Experimental reactor	160.3 ± 171	70 ± 68	7 ± 9	2.03 ± 1.4
Control 1 reactor	28.1 ± 5	1.2 ± 1.7	0.4 ± 0.6	1.17 ± 0.2

753

754

755 **Table S2.** Primers, probes and plasmid standards used in this study.

Primer-probe	Target	Plasmid standard	Sequence 5'-3'	References
BAC 1055F	Total Bacteria	*Geobacter sulfurreducens*	ATGGYTGTCGTCAGCT	[4]
BAC 1392R		(NC002939)	ACGGGCGGTGTGTAC	
BAC 1115 probe			CAACGAGCGCAACCC	
ARC 787F	Total Archaea	*Methanosarcina*	ATTAGATACC CSBGTAGTCC	[5]
ARC 1059R		*thermophila*	GCCATGCACCWCCTCT	
ARC 915F probe		(M59140)	AGGAATTGGCGGGGGAGCAC	
MBT 857F	*Methanobacteriales* (hydrogenotrophic)	*Methanobacterium formicium* (EU 544028)	CGWAG GGAAG CTGTT AAGT	[5]
MBT 1196R			TACCG TCGTC CACTC CTT	
MBT 929 probe			AGCAC CACAA CGCGT GGA	
MMB 282F	*Methanomicrobiales* (hydrogenotrophic)	*Methanomicrobiales KB 1-1* (AN – DQ301905)	ATCGR TACGG GTTGT GGG	[5]
MMB 832R			CACCT AACGC RCATH GTTTA C	
MMB 749 probe			TYCGA CAGTG AGGRA CGAAA GCTG	
MSC 380F	*Methanosarcinaceae* (mixotrophic)	*Methanosarcina thermophila* (M59140)	GAAAC CGYGA TAAGG GGA	[5]
MSC 828R			TAGCG ARCAT CGTTT ACG	
MSC 492 probe			TTAGC AAGGG CCGGG CAA	
MST 702F	*Methanosaetaceae* (acetoclastic)	*Methanosaeta KB 1-1* (AY 570685)	TAATC CTYGA RGGAC CACCA	[5]
MST 863R			CCTAC GGCAC CRACM AC	
MST 753 probe			ACGGC AAGGG ACGAA AGCTA GG	

756

757

758

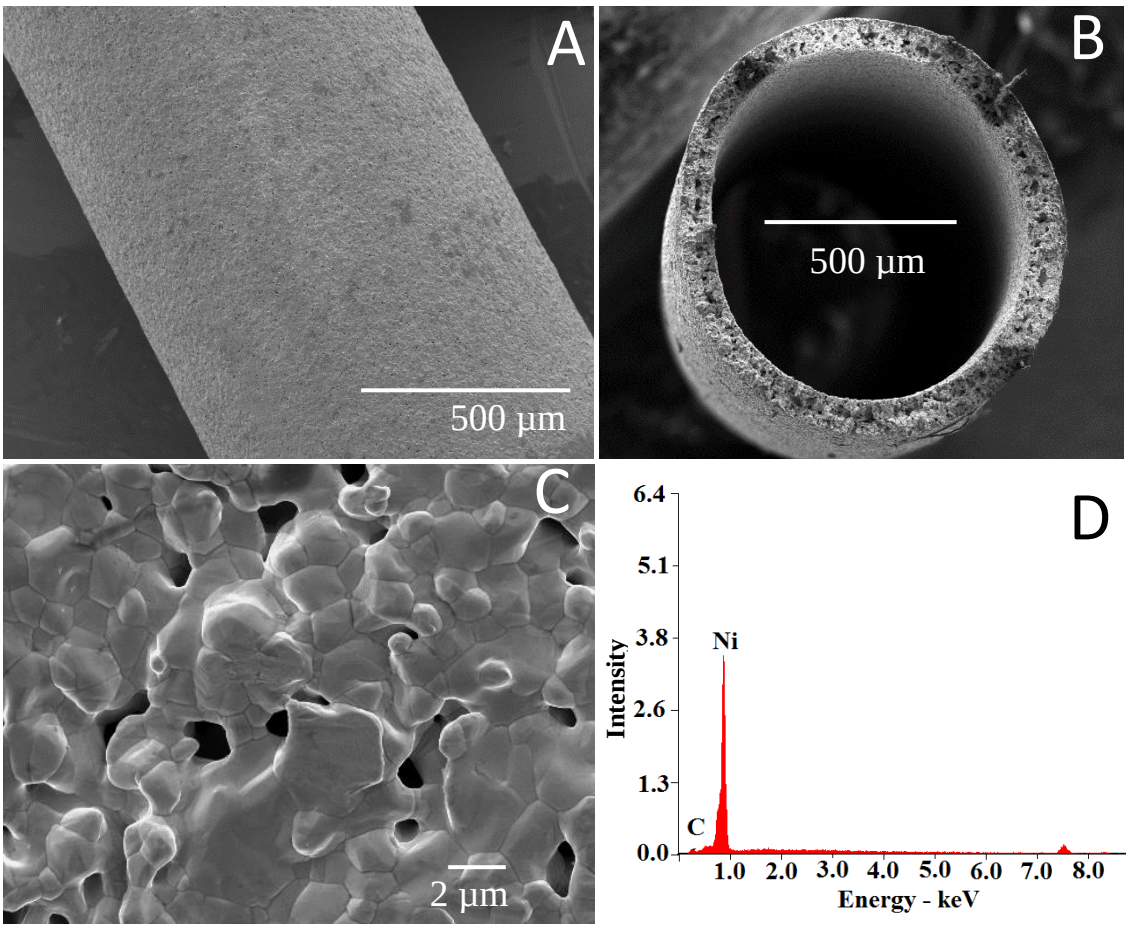

Figure S1. (A) Scanning electron microscope (SEM) image of the custom-built Ni-CCPHF cathode; (B) SEM image of the cross section of the Ni-CCPHF cathode; (C) SEM image of the surface of the Ni-CCPHF cathode; (D) Energy-dispersive X-ray spectroscopy (EDS) spectrum of the surface of the Ni-CCPHF.

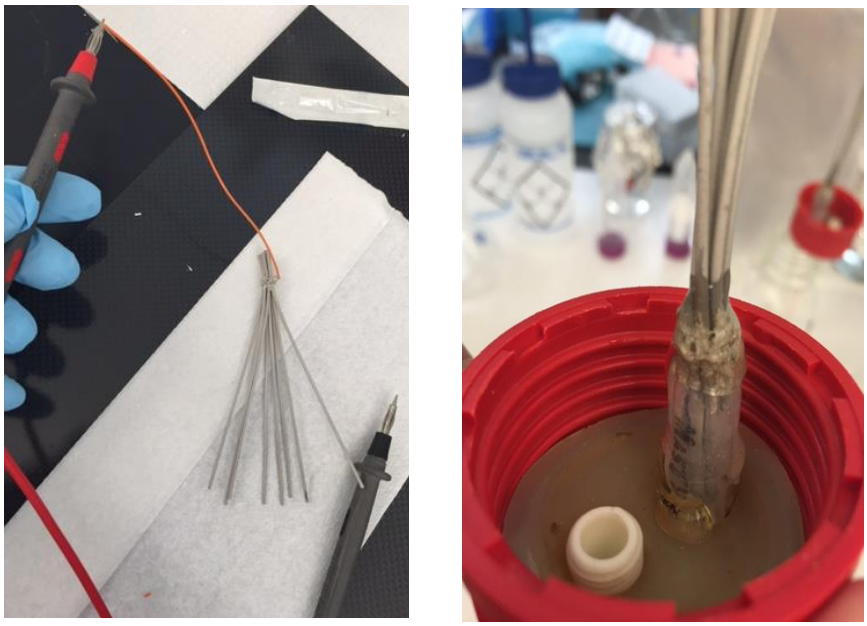

Figure S2. Image showing the hollow fibers prepared as a bundle and inserted into a polyethylene tube.

797 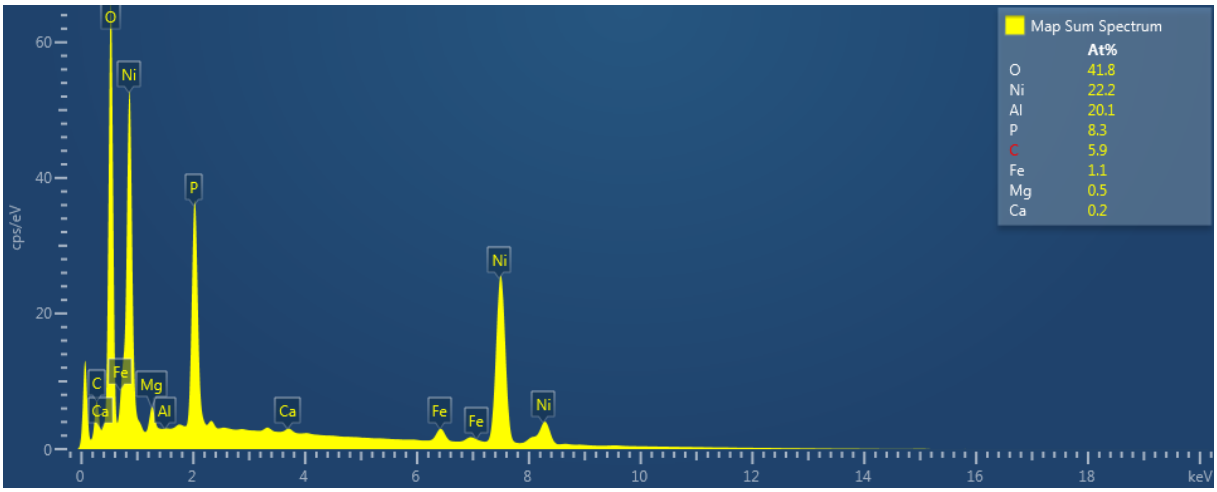

798 **Figure S3.** Energy-dispersive X-ray spectroscopy (EDS) spectrum of Ni-CCHF cathode that
799 served only as a cathode in control 1 reactor.

800

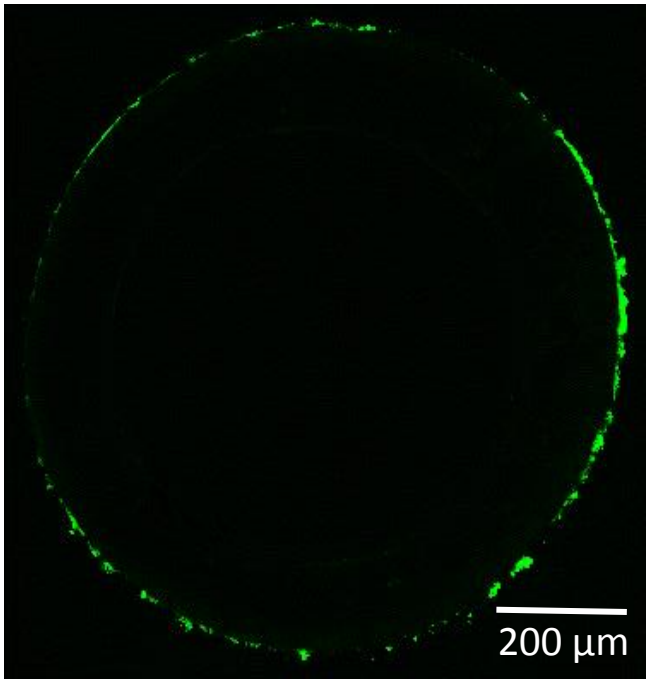

Figure S4. Confocal laser scanning microscope (CLSM) image (cross section) of cathodic biofilm developed on the Ni-CCPHF cathode of experimental reactor. The green color on the peripheral side of the Ni-CCPHF cathode represents microbial cells.

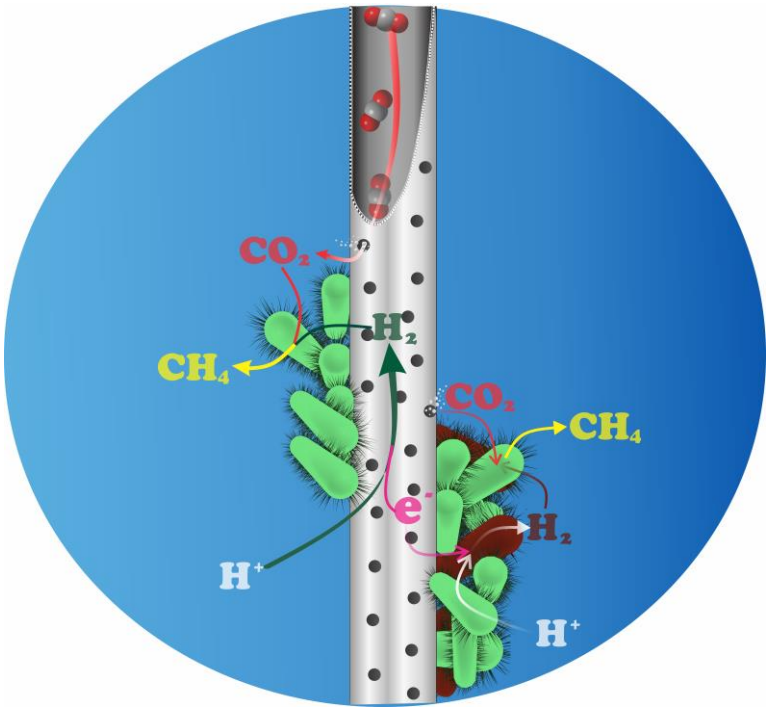

Figure S5. Schematic diagram representing possible bioelectrochemical reactions occurring on the surface of the Ni-CCPHF cathode of the experimental reactor. This schematic depicts CO_2 gas delivered directly to hydrogenotrophic methanogens through the pores of the hollow fiber cathode. The H_2 generated from hydrogen evolution reaction (HER) on the cathode surface is utilized by hydrogenotrophic methanogens for CH_4 generation. Also, this schematic depicts biotic H_2 generation by H_2 producing bacteria, and the biotic H_2 is consumed by hydrogenotrophic methanogens for CH_4 generation.

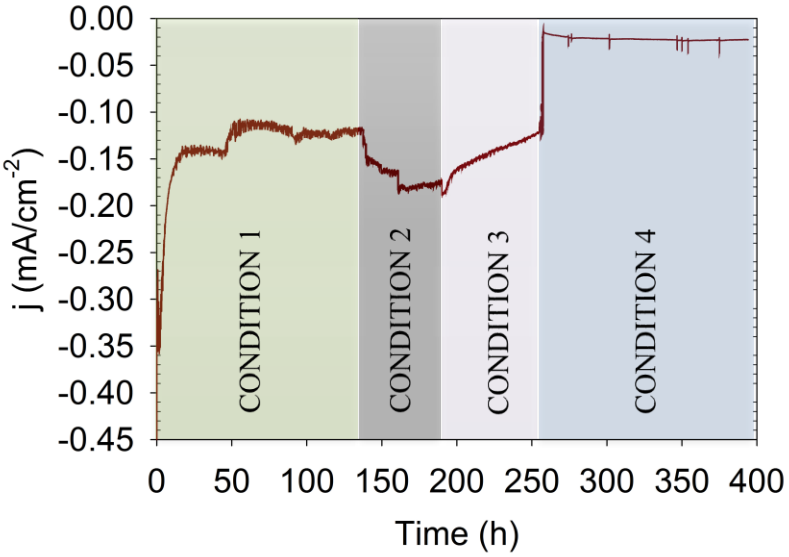

Figure S6. Amperometric current density over time for experimental reactor operated under different passive CO_2 concentrations (batch 9). Condition 1: 20% CO_2 and 80% N_2; Condition 2: 100% CO_2; Condition 3: 20% CO_2 and 80% N_2. Condtion 4: pure CO_2 gas was supplied in the reactor's headspace rather than through the pores of Ni-CCPHF cathode.

References

[1] a) B. Meng, X. Y. Tana, X. X. Menga, S. Z. Qiao, S. M. Liu, *J Alloy Compd* **2009**, 470, 461; b) K. P. Katuri, C. M. Werner, R. J. Jimenez-Sandoval, W. Chen, S. Jeon, B. E. Logan, Z. P. Lai, G. L. Arny, P. E. Saikaly, *Environ Sci Technol* **2014**, 48, 12833.

[2] K. P. Katuri, N. M. S. Bettahalli, X. B. Wang, G. Matar, S. Chisca, S. P. Nunes, P. E. Saikaly, *Adv Mater* **2016**, 28, 9504.

[3] a) J. R. Ambler, B. E. Logan, *Int J Hydrogen Energ* **2011**, 36, 160; b) A. R. Hari, K. P. Katuri, E. Gorron, B. E. Logan, P. E. Saikaly, *Appl Microbiol Biot* **2016**, 100, 5999.

[4] K. M. Ritalahti, B. K. Amos, Y. Sung, Q. Z. Wu, S. S. Koenigsberg, F. E. Loffler, *Appl Environ Microb* **2006**, 72, 2765.

[5] Y. Yu, C. Lee, J. Kim, S. Hwang, *Biotechnol Bioeng* **2005**, 89, 670.